# Two-dimensional Structure of the Light-harvesting Chlorophyll a/b Complex by Cryoelectron Microscopy

M. K. Lyon and P. N. T. Unwin

Department of Cell Biology, Stanford University School of Medicine, Stanford, California 94305

*Abstract.* The light-harvesting chlorophyll a/b complex (LHC-II) found in green plants has at least three functions: it absorbs light energy for transfer to the reaction centers, it is involved in keeping the photosynthetic membranes stacked, and it regulates energy distribution between the two photosystems. We have developed a procedure to produce large vesicles consisting almost exclusively of two-dimensional crystalline domains of LHC-II in which LHC-II is biochemically and structurally intact, as shown by SDS-PAGE, response to cations, and 77K fluorescence excitation spectra. The vesicles were examined by cryoelectron microscopy and analyzed, in projection, to a resolution of 17 Å. Their surface lattice consists of trimers arranged in interlocking circles; the two-sided plane group is p321 (unit cell dimension, $a$ = 124 Å) with two, oppositely facing trimers/unit cell. Individual trimers consist of matter arranged in a ring, around a central cavity, an appearance similar to that obtained in some conditions using negative stain (Li, J., 1985. *Proc. Natl. Acad. Sci. USA.* 82:386–390). The monomer (~45 × 20 Å) is seen as two domains of slightly different size at this resolution. The thickness of single layers is ~48 Å, measured from edge-on views of the frozen vesicles. Based on these dimensions, the molecular mass of the monomer is ~30 kD. Therefore, each monomer appears to be composed of a single polypeptide and its associated pigments.

THE light-harvesting chlorophyll (chl)[1] a/b complex (LHC-II) associated with photosystem II in green plants is the most abundant protein complex in photosynthetic membranes (31). LHC-II absorbs solar energy for transfer to the photosystems, is involved in maintaining the stacked arrangement of grana, and regulates energy distribution between the photosystems (for reviews, see references 2, 3, 23). In vitro, cations, particularly magnesium, are required for LHC-II to maintain the stacked organization of thylakoids, while, in vivo, phosphorylation of LHC-II controls energy distribution between photosystems I and II (2).

In the last few years, information has accumulated regarding the structure of this complex. It has two major polypeptides, derived from a multigene family (9), with molecular masses of ~26 and 29 kD, which noncovalently bind chlorophylls a and b, and xanthophylls (2, 3, 27). Classes of monoclonal antibodies have been developed that bind both of the major polypeptides, while other classes of monoclonal antibodies react with one but not the other polypeptide, suggesting that the 26- and 29-kD polypeptides have common, but not identical, structural features (6). The 26-kD polypeptide may have three transmembrane α helical segments, according to hydropathy plots (13). On nondenaturing gels, LHC-II can be found as an oligomer (2, 3). However, it is not known whether LHC-II complexes consist of oligomers of a single type of polypeptide, or whether both the 26- and 29-kD polypeptides are found in each complex. It has been suggested that there may be two or more classes of complexes, depending on the ratios of the two polypeptides making up the complex, and that one class of LHC-II may be tightly associated with photosystem II, while a second class may be more mobile and more readily phosphorylated (8, 18).

Projection maps and three-dimensional structures have been determined for two-dimensional crystals of LHC-II complexes produced in reconstituted membranes (19, 20) and without reconstitution into membranes (15, 16). The two reconstructions share certain similarities, both showing trimers arranged in alternating orientation on a p321 lattice with a unit cell dimension of ~120 Å (14, 16, 19, 20). However, the shape of the trimers appears different in the two reconstructions.

One of the major difficulties in attempting to form crystals of LHC-II complexes has been the tendency of the lattices to form multilayers, or "stack", in response to cations (14, 16, 19, 20). It is difficult to use electron micrographs of the multilayers for image analysis and reconstruction. Recently, a procedure has been developed for obtaining three-dimensional crystals of LHC-II complexes (15). However, these

M. K. Lyon's present address is Department of Molecular Biology MB14, Scripps Clinic and Research Foundation, 10666 North Torrey Pines Road, La Jolla, CA 92037. P. N. T. Unwin's present address is Medical Research Council Centre, Laboratory of Molecular Biology, Hills Road, Cambridge CB22QH, England.

1. *Abbreviations used in this paper*: chl, chlorophyll; LHC-II, chlorophyll a/b light-harvesting complex associated with photosystem II.

crystals appear to be either too small or insufficiently ordered for x-ray analysis (15). To circumvent these problems, we have developed a new procedure for obtaining two-dimensional crystals of LHC-II, and report here on their properties and structure.

## Materials and Methods

### Isolation and Crystallization

LHC-II was isolated from market spinach by the method of Burke et al. (5) with the modification that phenylmethylsulfonyl fluoride was added to the isolation buffer just before use. The final pellet had a chl a/b ratio of ~1.20:1 and was resuspended in 2 mM EDTA (free acid), 10 mM Tris base pH 6.4 with a tissue homogenizer. The chlorophyll concentration was adjusted to 1.0–1.5 mg/ml. 10% (wt/vol) Triton X-100 (Boehringer Mannheim Biochemicals, Indianapolis, IN) was added in 25-μl aliquots until the suspension appeared clear. The sample was examined by light microscopy at 400× and appeared as a clear green solution with no particulate material. Dialysis of 250–500 μl of sample was against 1800 ml of 2 mM EDTA, 1 mM Na azide, 10 mM Tris base pH 6.4 at room temperature, with stirring and protection from light. Dialysis buffers were changed one to two times daily, and crystallization occurred within 3–6 d. Chlorophyll concentrations were determined as previously described (1).

### Trypsin Treatment and Electrophoresis

Trypsin treatment was for 10 min at room temperature, followed by 10 min incubation with trypsin inhibitor, at the concentrations given in Fig. 2. Samples were then pelleted and resuspended in SDS sample buffer. (trypsin type XI, trypsin inhibitor type II-S, Sigma Chemical Co., St. Louis, MO.) SDS-PAGE was at room temperature in a minigel apparatus (Hoeffer, Scientific Instruments, San Francisco, CA) using the Laemmli system (17). The sample buffer was 62.5 mM Tris base pH 6.8, 2% SDS, 5% 2-mercaptoethanol, and 10% glycerol.

### Fluorescence Microscopy and 77K Fluorescence Spectra Measurements

Two-dimensional crystals were examined and photographed on a Zeiss fluorescence microscope. For fluorescence, the excitation range was 450–490 nm, while the emission range was 530 nm and above, with a maximum at 550 nm. Samples were photographed with Kodak Tri-X shot at ASA 1600 and developed in Diafine. Fluorescence spectra were obtained under liquid nitrogen as previously described (26).

### Electron Microscopy

For preliminary examination of preparations, 5-μl aliquots of sample were applied to freshly prepared and glow-discharged carbon films on 400 mesh copper grids (Ernest F. Fullam, Inc., Schenectady, NY). After ~2 min,

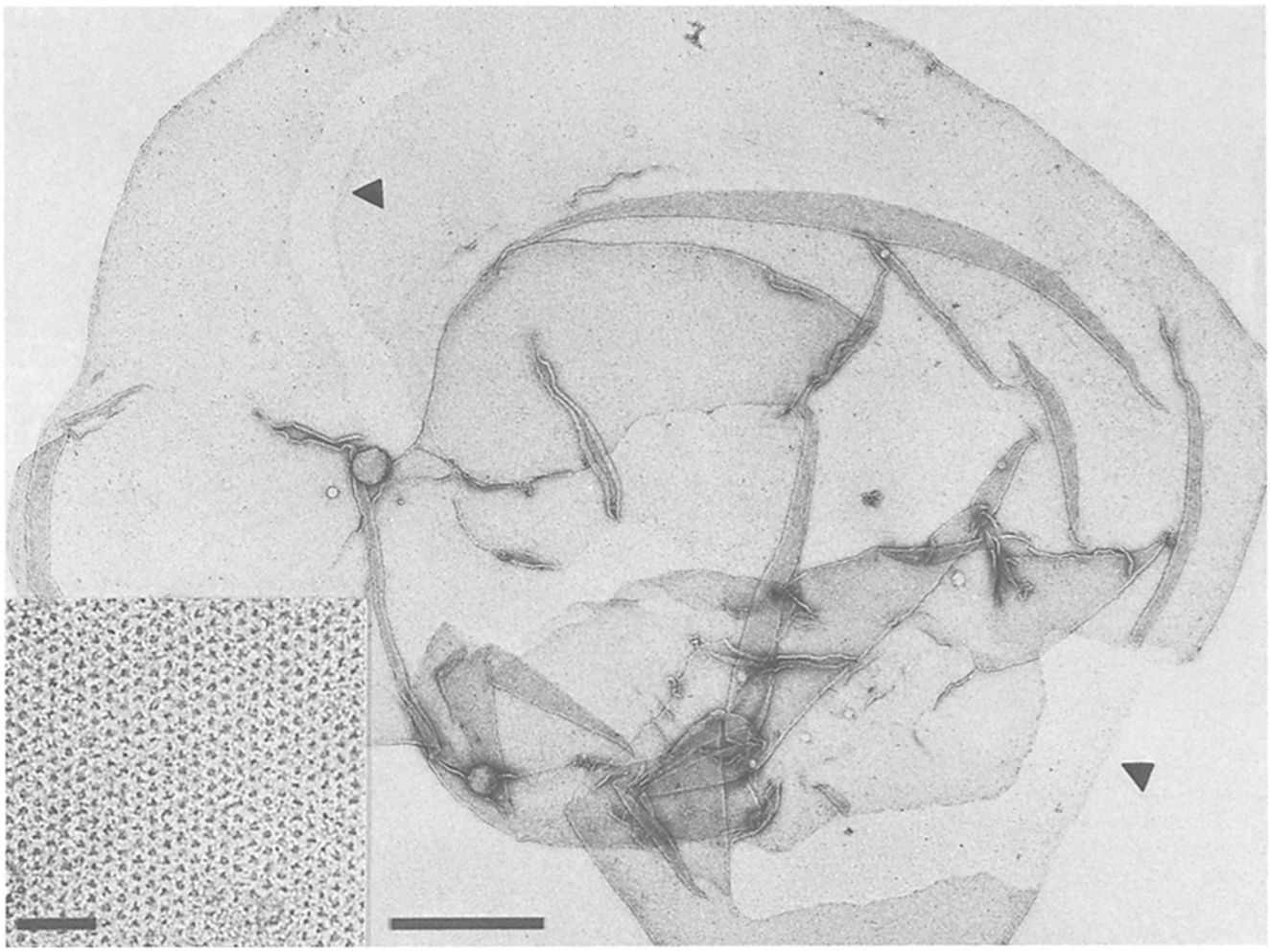

*Figure 1.* Collapsed vesicle with LHC-II crystalline arrays. A single side of the vesicle can be seen in areas where the vesicle has broken open (*arrowheads*). Bar, 0.59 μm. (*Inset*) Higher magnification view, showing characteristic hexagonal spacing of holes in the lattice. Bar, 0.05 μm. Samples stained with 2% uranyl acetate.

grids were washed in double-distilled water and stained with 2% uranyl acetate. For staining with $OsO_4$ vapor, 5-μl aliquots were applied as above, blotted briefly, and allowed to dry in a petri dish with several drops of 2% aqueous $OsO_4$ in the chamber. For freezing, holey carbon films were prepared and samples were frozen in liquid ethane as previously described (21). Vesicles over holes were located by examination of underfocused images at 3,600×. Low dose cryoelectron microscopy was done using a Philips EM400T with a cryoholder (Gatan, Inc., Pleasanton, CA). All micrographs were taken at 36,000× at ~8,000 Å defocus, as calibrated by the Thon ring pattern from the carbon film (30). The objective lens current was noted and calibration was accomplished by photographing catalase crystals under similar conditions. Thickness measurements were made of edge-on views enlarged to 250,000×, using a calibrated 7× magnifier.

### *Image Processing*

Electron micrographs were selected for analysis by examining their optical diffraction patterns for two criteria. First, they were required to show strong, sharp reflections, extending in all directions to at least the third order. Secondly, the diffraction patterns derived from the two sides of a vesicle had to be well separated, so that individual reflections did not overlap. Micrographs were scanned with a microdensitometer (Perkin-Elmer Corp., Eden Prairie, Mn) using step and aperture sizes of 25 μm. The typical array size was ~525 × 425 pixels. Processing was done with a set of programs developed originally at the Medical Research Council, Cambridge, England. Filtered images were computed and those showing discontinuities or other faults were discarded. Projection maps were synthesized from the scanned arrays as in (11), using background subtracted, sinc-weighted amplitudes (12).

## *Results*

Purified, solubilized LHC-II complexes were dialyzed against a low salt buffer with EDTA, in order to prevent either precipitation of LHC-II or the formation of multilayers, both of which occur in the presence of cations (16, 20). With EDTA in the dialysis buffer, large vesicles were formed which consisted almost entirely of ordered domains (Fig. 1). The vesicles were made of a single layer, as could be seen where they were broken open. The entire preparation consisted of these crystalline vesicles, with very little precipitate. Most of the vesicles collapsed on electron microscope grids, rather than breaking open, so that micrographs included two layers of crystalline areas. The vesicles tended to be oblong, with measurements of 3.13 ± 0.66 × 1.75 ± 0.58 μm (average of 10 measurements, ±SD).

The crystallization process itself occurred under a fairly narrow range of conditions. Crystals were obtained only when the purified LHC-II had a chl a/b ratio of 1.20:1–1.18:1 and was resolubilized with a detergent/chl ratio of 10:1–20:1 (wt/wt). Crystallization occurred between 3 and 6 d of dialysis. If the chl a/b ratio was <1.18:1, resolubilization could only be accomplished with much greater quantities of detergent, and dialysis then yielded a fine precipitate. If the chl a/b ratio was >1.20:1, dialysis yielded multilayer sheets with little apparent order. In both crystalline and noncrystalline preparations, the polypeptide content appeared similar.

### *Biochemical Characterization*

The preparations were characterized by SDS-PAGE, by examination of low temperature fluorescence spectra, and by response to cations. SDS-PAGE showed that the vesicles consisted of two polypeptides of ~24 and 27 kD, with the larger polypeptide being more abundant (Fig. 2, lane *2*). When the sample was not boiled in SDS buffer, a green band was observed at ~34 kD (Fig. 2, *arrow*, lane *4*), which is characteristic of monomers of LHC-II which have retained chlorophyll (7, 8). In addition, a green band was also observed at ~81 kD (Fig. 2, *arrow*, lane *4*), which presumably consisted of an oligomer of LHC-II units with chlorophyll. The appearance of an additional band in the 24–27-kD region under these conditions probably reflects an incomplete loss of pigments from the polypeptides, resulting in slight variations in molecular masses, as reported earlier (7). An aliquot of crystals was also treated with trypsin (Fig. 2, lanes *6* and *7*), which led to a slight decrease in molecular mass. Similar results have been observed in several laboratories when unstacked thylakoids were treated with trypsin (2, 3).

Fluorescence excitation spectra at 77K were examined with three preparations (Fig. 3). In vivo, the major peaks of light absorption and fluorescence of the pigments associated with LHC-II overlap, which allows energy to be transferred in a specific manner from xanthophylls and chl b to chl a. The peak fluorescence of chl a is at 680 nm (27). By illuminating the samples with wavelengths absorbed by each of the three pigment groups and examining fluorescence at

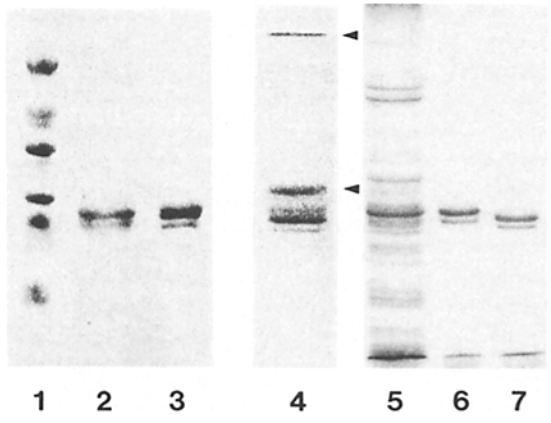


*Figure 2.* SDS-PAGE of crystalline LHC-II. Lane *1*, molecular mass standards (from top: 66, 45, 36, 29, 24, and 20.1 kD). Lane *2*, crystalline LHC-II, heated. Lane *3*, LHC-II before crystallization, heated. Lane *4*, crystalline LHC-II, not heated. Arrows indicate bands that were green before staining with Coomassie Blue. Lane *5*, thylakoids. Lane *6*, crystalline LHC-II. Lane *7*, similar aliquot of crystalline LHC-II as in lane *6* after incubation with 0.1 μg trypsin, followed by 0.2 μg trypsin inhibitor. Samples in lanes *5–7* were heated in SDS sample buffer. Lanes *1–3*, 13.5% polyacrylamide gel. Lanes *4–7*, 14% polyacrylamide gel.

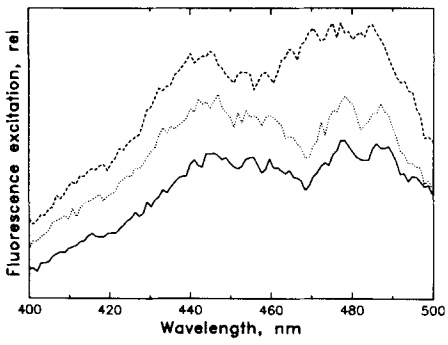


*Figure 3.* 77K excitation spectra. The relative fluorescence was monitored at 680 nm while samples were illuminated from 400 to 500 nm. Curves 1-3 are three preparations of crystalline LHC-II: (———) curve 1; (· · · ·) curve 2; (- - - -) curve 3.

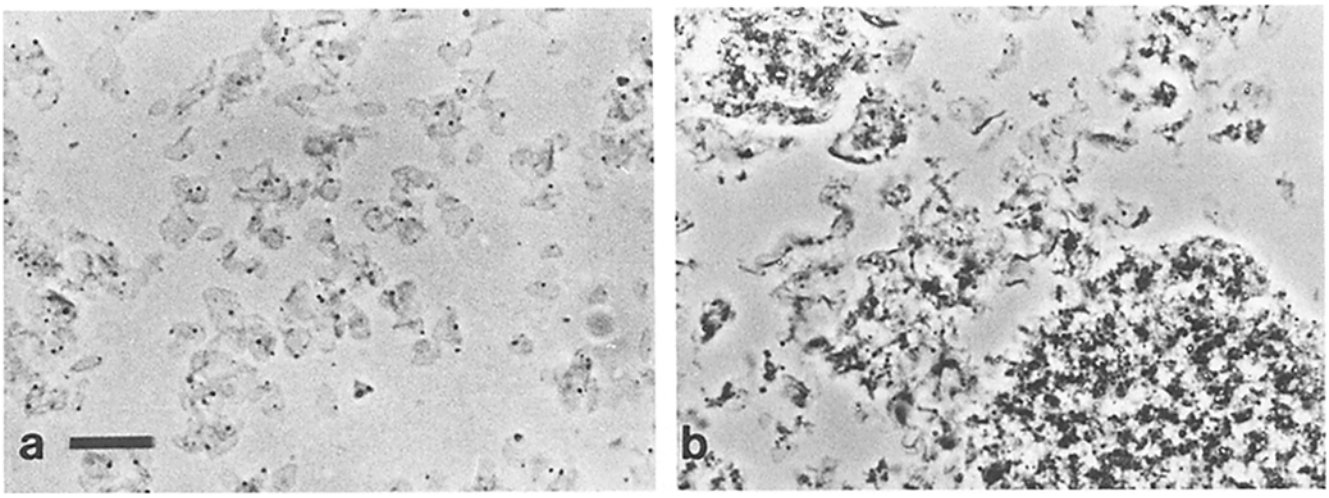


*Figure 4.* (*a*) Light micrograph of LHC-II vesicles in 2 mM EDTA. Almost all such vesicles consisted of crystalline LHC-II, as determined by electron microscopy. In EDTA, the vesicles are flat and show little aggregation. (*b*) Same sample as in *a* after dialysis against 4 mM $MgCl_2$. Vesicles are clumped into large aggregates. Bar, 10.2 μm.

680 nm, it is possible to determine if energy is transferring from the xanthophylls and chl b to chl a (26, 27). The 680-nm fluorescence of three preparations of LHC-II vesicles is shown in Fig. 3. The peak absorbances are 440 nm for chl a, 470 nm for chl b, and 450–490 nm for the various xanthophylls. While all three preparations show chl a fluorescence in the range where chl b and the xanthophylls are being activated (450–490 nm), curve 3 (- - - -) shows the most complete transfer of energy from chl b and the xanthophylls to chl a, suggesting that the pigments have remained in their correct orientations. All image analysis reported here was done with this particular preparation. Vesicles were also examined by fluorescence microscopy, with excitation at 450–490 nm. The fluorescence observed was in the red range, with no visible background fluorescence.

By light microscopy, vesicles in dialysis buffer appeared flat, with only minor clumping or aggregation (Fig. 4 *a*). However, after dialysis against 10 mM Tris base pH 6.4, 4 mM $MgCl_2$ for 1 h, the vesicles were clumped into large aggregates (Fig. 4 *b*).

### *Negative Stain Electron Microscopy*

Samples were routinely examined by negative staining with 2% uranyl acetate (Fig. 1, *inset*). However, the appearance of the arrays was variable under these conditions. In some areas of the microscope grid, an hexagonal array of black spots, or stain deposits, was visible (Fig. 1 *inset*) whereas in other areas, an array of white spots, or stain exclusion areas, was observed (Fig. 5 *a*). If a very low concentration of Triton X-100 was included in the uranyl acetate, as in (14), the stain deposits were predominant. Some areas appeared to have no order when observed near focus (Fig. 5 *b*), but clearly showed order when the same image was defocused (Fig. 5 *c*). If samples were exposed on the grid to $OsO_4$ vapors (Fig. 5 *d*), which primarily stains lipid (10), a pattern similar to that shown in Fig. 1, (*inset*) was found, suggesting that lipid surrounds portions of the protein.

Some of this variation in appearance is probably due to variation in the deposition of stain. Incomplete penetration of the stain could give the appearance of a relatively flat surface, as seen in Fig. 5, *b* and *c* (compared with Fig. 1, *inset*). In addition, some of the variation may be due to differences in the composition of the unit cell. For example, if lipid molecules were to associate with each of the large cavities (see Fig. 1, *inset*), patterns of stain exclusion would result, as seen in Fig. 5 *a*.

### *Cryoelectron Microscopy and Image Processing*

For cryoelectron microscopy, the vesicles in dialysis buffer were rapidly frozen over holey carbon films and thus were in a hydrated state with no stain or fixative present. The images were essentially featureless at the defocus level used (~8,000 Å, Fig. 6).

Occasionally, an edge-on view was obtained (Fig. 6, *inset*). The average thickness of the crystals, estimated from 12 such views by measuring from the outer edges of each dark line, was 48 Å (SD = ±4).

Although images of the crystalline vesicles were featureless, their diffraction patterns showed reflections that could be indexed according to two separate reciprocal lattices (see Fig. 7, where the two lattices are rotated relative to each other by an angle of approximately 7°). There was no specific relationship between lattices on each side of a collapsed vesicle, as the angle of rotation varied from vesicle to vesicle. By applying masks to each of the reciprocal lattices, filtered images of each side of the vesicle containing a single crystalline layer could be synthesized. These showed that the structure was a set of interlocking rings, each consisting of six triangular shapes.

Projection maps obtained with no symmetry imposed (Fig. 8) suggest that the two-sided plane group of the surface lattice is p321, in agreement with earlier findings on related structures (14, 19). The average phase errors (±SD) associated with three possible symmetries, using the nine images analyzed, were: p6, 17.2 ± 2.7; p3, 14.5 ± 1.4; p321, 14.3 ± 1.4. The appearance departs from sixfold at higher resolution and there is an obvious indication of a mirror plane, as

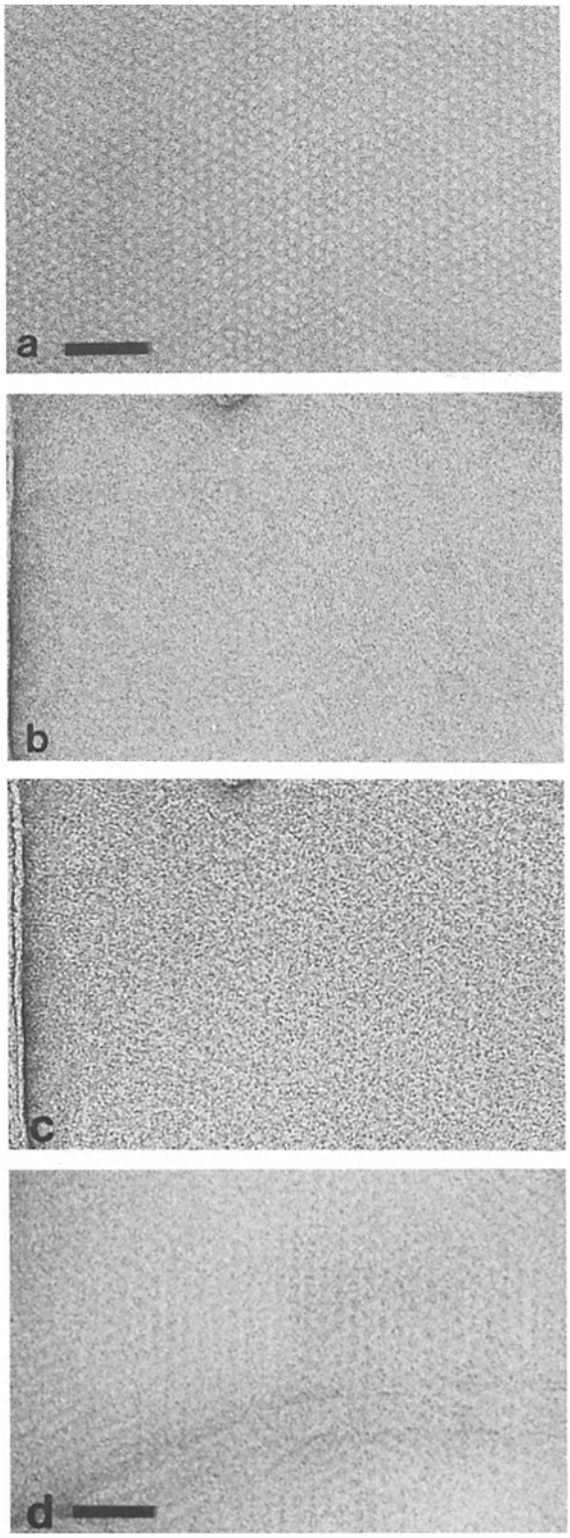


*Figure 5.* (*a*) Area of LHC-II crystals which were stained in 2% uranyl acetate under the same conditions as inset, Fig. 1. (*b*) Area of LHC-II crystals stained with 2% uranyl acetate. Image is just slightly underfocused and no ordered structure is visible. (*c*) Same area as *b* but more underfocused. Ordered structure is clearly visible. (*d*) Area of LHC-II crystals stained with $OsO_4$ vapor. Bars: (*a–c*) 0.05 μm; (*d*) 0.07 μm.

would be obtained with a twofold axis parallel to the plane of the membrane.

A projection map (resolution 17 Å) with p321 symmetry imposed was synthesized from the structure factors averaged from the nine images (see Fig. 9; Table I). The unit cell (dimension, $a$ = 124 Å [SD = ±3 Å]) contains two oppositely facing trimers. The large circle formed by six trimers has an outer diameter of 190 Å, while the diameter of the central open space is ~68 Å at its narrowest point and 95 Å at the widest point. Individual trimers consist of protein arranged in a ring around a central cavity. Within the trimer, there are alternating domains of slightly different size (*a* and *b* in Fig. 9). Based on the extent of connection between domains, the monomer probably consists of the two domains indicated in Fig. 9. The projected area occupied by the monomer (from the zero level contour) is ~900 Å$^2$. Assuming the measured thickness of 48 Å and a partial specific volume of 1.3 Å$^3$ per dalton (32), it has a molecular mass of ~30 kD.

## Discussion

### Formation of Two-dimensional Crystals

The formation of crystals of LHC-II in the presence of EDTA is probably due to hydrophobic interactions, since the crystals develop as a result of depletion of detergent rather than changes in salt conditions. The nature of the trimer–trimer associations seen in the projection maps (Fig. 9) from the ice-embedded specimens is consistent with this situation. Each trimer is surrounded by three other trimers, with a close association over an extended region. These regions are likely to include the hydrophobic, membrane spanning portions of the complex, since this part of the structure is strongly contrasted in ice.

### Comparison with Reconstructions in Negative Stain

Two three-dimensional reconstructions of LHC-II have been published (14, 19). While there are many agreements be-

*Table I. List of Structure Factors for p321 Projection Map**

| *h,k* | Amplitude | Phase‡ |
|---|---|---|
| 1,0 | 112.0 | 360 |
| 1,1 | 67.0 | 143 |
| 2,0 | 67.1 | 180 |
| 1,2 | 82.4 | 181 |
| 3,0 | 177.9 | 360 |
| 2,2 | 64.4 | 335 |
| 1,3 | 78.2 | 215 |
| 4,0 | 67.6 | 360 |
| 2,3 | 74.7 | 50 |
| 1,4 | 70.8 | 219 |
| 5,0 | 65.7 | 180 |
| 3,3 | 64.7 | 79 |
| 2,4 | 43.7 | 259 |
| 3,4 | 54.0 | 209 |
| 2,5 | 45.9 | 27 |

* Obtained from nine images, each consisting of 500–1,100 unit cells.
‡ In degrees; average phase errors, based on comparison of individual phases with the threefold related phases were: 10.5, 14.3, 14.0, 16.6, 13.0, 12.2, 15.8, and 14.9.

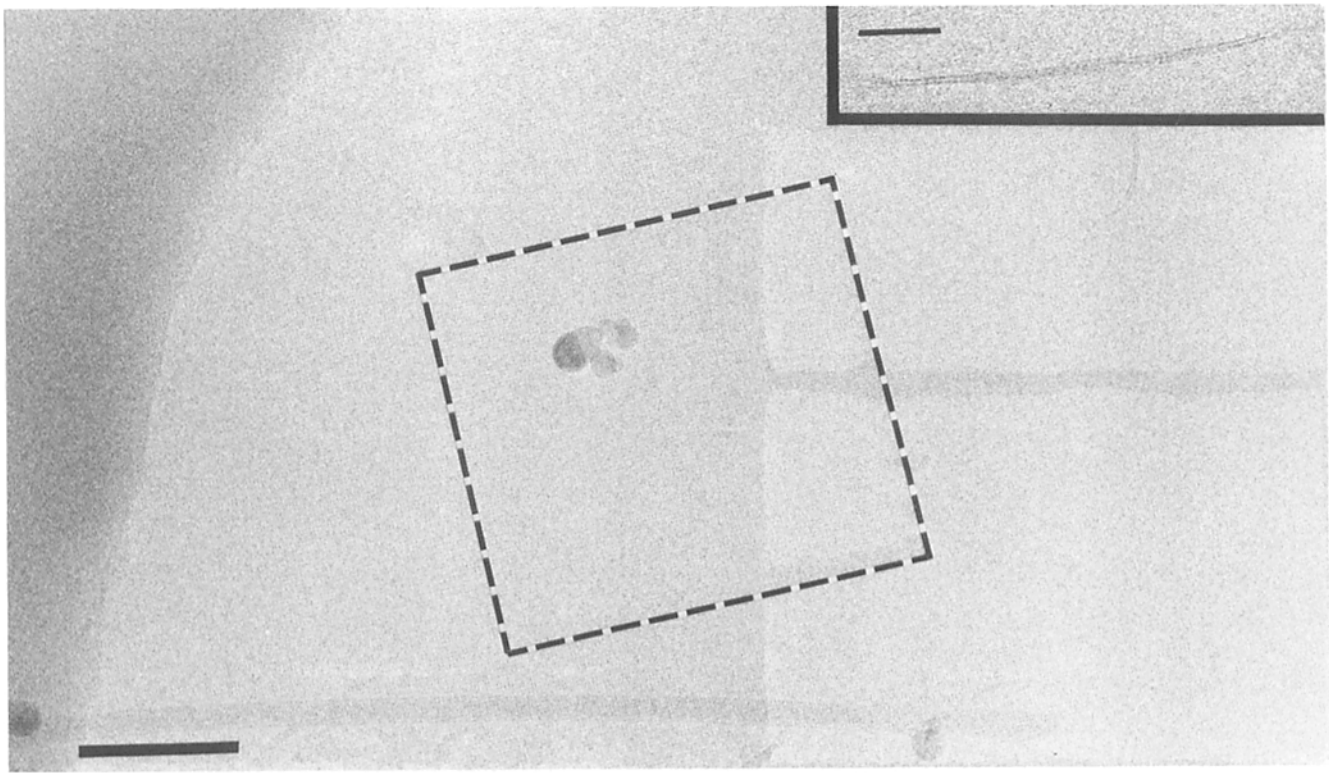

*Figure 6.* LHC-II vesicle in ice over hole in carbon film. Dashed line indicates an area which was scanned. Bar, 0.10 μm. (*Inset*) Edge-on view. Bar, 0.05 μm.

tween those reconstructions and this analysis, there are also differences. All three structures possess p321 symmetry and the unit cell sizes are essentially the same. All three crystals have an arrangement of six units around a central open space of about the same size. With other features, there is less consistency. The thickness of the crystals has been determined as 48 (this work), 60 (15), and 70 Å (20). In addition, planar aggregates of LHC-II have a reported thickness of 51 Å (20). The variation may be due to the techniques that were used to measure the thickness, which included direct measurement in ice (this work), measurements of metal-shadowed material (14), x-ray diffraction of lattices of LHC-II alone, and LHC-II arrays reconstituted into membranes (20). A second source of variation in thickness is the amount of lipid associated, as previously suggested (20).

Another difference between this analysis and previous reconstructions lies in the apparent organization of the monomers. In the present study, three monomers are associated in a "head-to-tail" fashion around a central cavity, and the central cavity has three lobes that are slightly twisted, giving it a slight handedness. In contrast, one of the reconstructions (14), which was also determined at 17 Å resolution, appears to show a different arrangement. In that case, the monomers are joined at only one end, forming a "three-armed" trimer with a central density instead of a central cavity. In the other reconstruction (19), the trimers show features that are similar to those found here, although the resolution (30 Å) makes direct comparison difficult.

There are two possible reasons for the differences between the structures in projection. First, biochemical factors may be involved, as each study used a distinct crystallization procedure and the ratio of the two polypeptides varies in each case. Secondly, the methods used to examine the crystals may be an important factor. This analysis was done with samples in a frozen, hydrated state, while all previous work was done using negative stain. Because all three studies are in agreement with regard to the crystal symmetry and unit cell size, it seems most likely that the differences are due to the second factor, the method of examining the crystal. It is possible that in some circumstances stain is unable to penetrate the small cavity formed by the three monomers, thus giving rise to a misleading representation of the true structure.

### *Relationship between Crystalline and Native LHC-II*

LHC-II complexes in the two-dimensional crystals are functionally intact. Two polypeptides were found, with apparent molecular masses of 24 and 27 kD. These masses are slightly less than some reported in the literature, but the discrepancy is more likely the result of the anomalous behavior of pigment-binding proteins on SDS-PAGE (7) than to proteolysis. LHC-II in intact thylakoids responds to the presence of cations by causing the membranes to stack, a process that only occurs if the LHC-II polypeptides are intact, particularly with respect to the $NH_2$ terminus (2, 3, 22, 28). Vesicles of crystalline LHC-II responded to cations by aggregating in a manner similar to the stacking of intact thylakoids. In addition, trypsin treatment of crystalline LHC-II (Fig. 2) gave results that appear identical to trypsin treatment of thylakoids (2, 3, 22, 28). However, these results do not exclude the possibility of proteolysis at the COOH terminus.

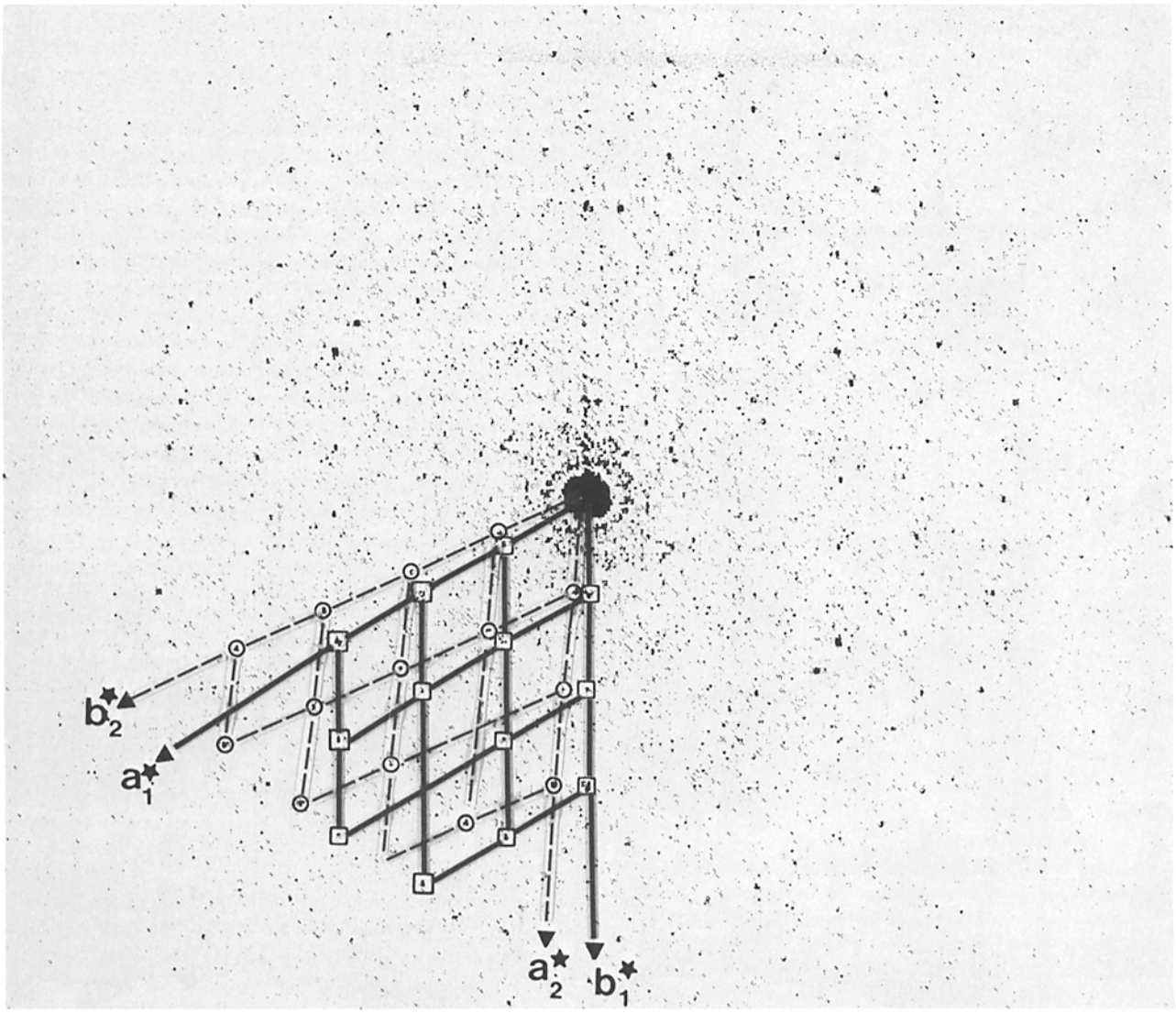


*Figure 7.* Computed diffraction pattern of the area scanned in Fig. 6. Diffraction patterns from two lattices can be seen, with reflections of one lattice indicated by squares and reflections of the opposite facing second lattice indicated by circles. The angle of rotation between the two lattices is ~7°. Reciprocal lattice vectors ($a_1^*$, $h_1^*$) and ($a_2^*$, $b_2^*$) are indicated for each lattice.

The presence of green bands on SDS gels under mild electrophoretic conditions showed that pigments were bound by the polypeptides. More importantly, by examining 77K fluorescence excitation spectra, it was possible to determine that all pigments associated with LHC-II (chl a, chl b, and xanthophylls) were not only present, but functionally intact. It has recently been suggested that the xanthophylls are in fact required for the stable association of chlorophylls a and b with LHC-II polypeptides (25). This may explain some of the difficulties in forming two-dimensional crystals, as the xanthophylls are the most detergent-sensitive component of the complex (27). Their presence or absence would not be detected either by SDS-PAGE or the determination of the chl a/b ratio.

SDS-PAGE revealed that there were unequal amounts of two polypeptides in the LHC-II lattices. The monomers seen in the projection map have an estimated molecular mass of 33 kD, based on the measured thickness of the crystals in ice. Even if other thickness measurements are used (14, 20), the maximum molecular mass of the monomers would be ~48 kD, which is probably not large enough to include two polypeptides. Thus, it is unlikely that the monomers include more than a single polypeptide. The same conclusion was reached in one of the previous studies (14). LHC-II polypeptides have considerable homology (9) and, therefore, are likely to have similar tertiary organization. It is possible that they can fit into the crystal in an interchangeable manner, and it is an average view that is presented in the projection maps, as suggested previously (14). Alternatively, only one of the polypeptides has crystallized, and the second polypeptide remains in noncrystalline areas of vesicles.

There is only indirect evidence that LHC-II complexes in thylakoids are arranged in trimers. Numerous studies have shown that purified LHC-II gives freeze-fracture particles of ~80 Å (3), a size that is compatible with the trimers found in this study. In addition, oligomeric forms of LHC-II are detected with nondenaturing gel electrophoresis (3, 8, 27). It does appear that crystalline LHC-II is functionally equiva-

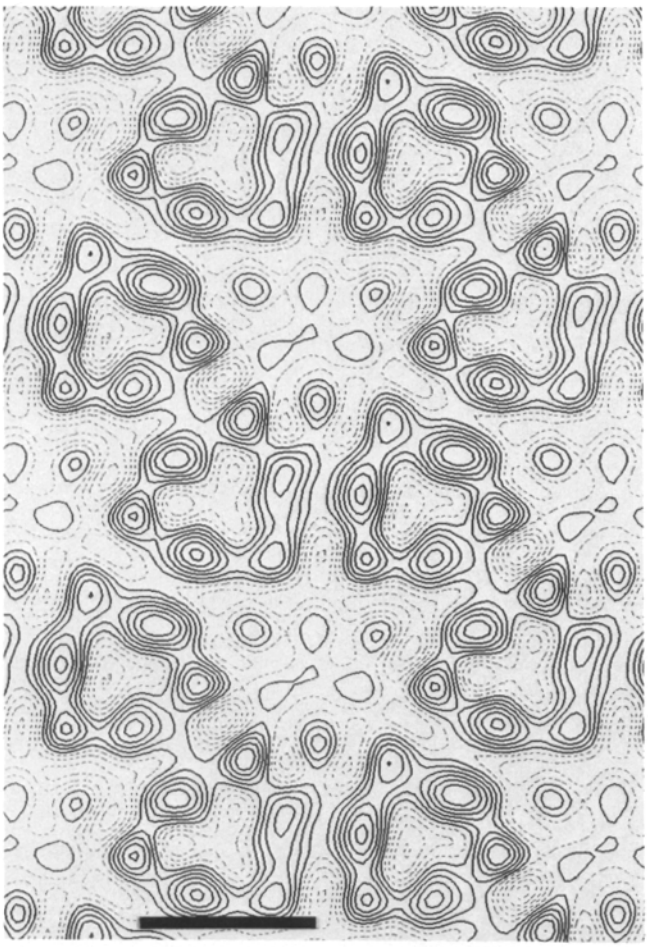

*Figure 8.* Projection map of a single crystal, with no symmetry imposed. Solid contours represent regions of higher density (i.e., protein). Trimers of protein are arranged in groups of six to form interlocking circles, two of which are shown here. Bar, 60 Å.

lent to freshly isolated LHC-II, based on cation response, SDS-PAGE, and fluorescence excitation. Low temperature linear dichroism studies have given evidence that pigment orientation is probably not changed with solubilization and purification of LHC-II (29). However, it is still possible that the oligomeric forms of LHC-II reflect hydrophobic interactions which occur in the presence of detergent, rather than being the native structure of LHC-II in thylakoids.

Experimental evidence has shown that the COOH- and $NH_2$-terminal ends are on opposite sides of the membrane (3, 4) and that there are probably three to five membrane-spanning α helices in each polypeptide (24). A specific model, based on hydropathy plots, predicts that there are three α helices extending through the membrane (4, 9). At a resolution of 17 Å, α helices cannot be distinguished. However, the total area occupied by the two domains of the monomer is quite large (~900 $Å^2$) suggesting that there are at least three membrane-spanning α helices, and likely to be more.

Special thanks to Dr. Jeanette Brown, Carnegie Institute of Washington, Stanford, California, for obtaining the 77K excitation spectra. We would like to thank our colleagues at Stanford University for their invaluable advice and discussion during the course of this work.

This study was supported by National Research Service Award GM 10835-02 to M. K. Lyon and National Institutes of Health grant GM 27764 to P. N. T. Unwin.

Received for publication 2 November 1987, and in revised form 22 January 1988.

***References***

1. Arnon, D. I. 1949. Copper enzymes in isolated chloroplasts. *Plant Physiol.* 24:1–15.
2. Bennett, J. 1983. Regulation of photosynthesis by reversible phosphorylation of the light-harvesting chlorophyll a/b complex of lettuce chloroplasts. *Biochem. J.* 212:1–13.
3. Brecht, E. 1986. The light-harvesting chlorophyll a/b-protein complex: results from a twenty-year research period. *Photobiochem. Photobiophys.* 12:37–50.

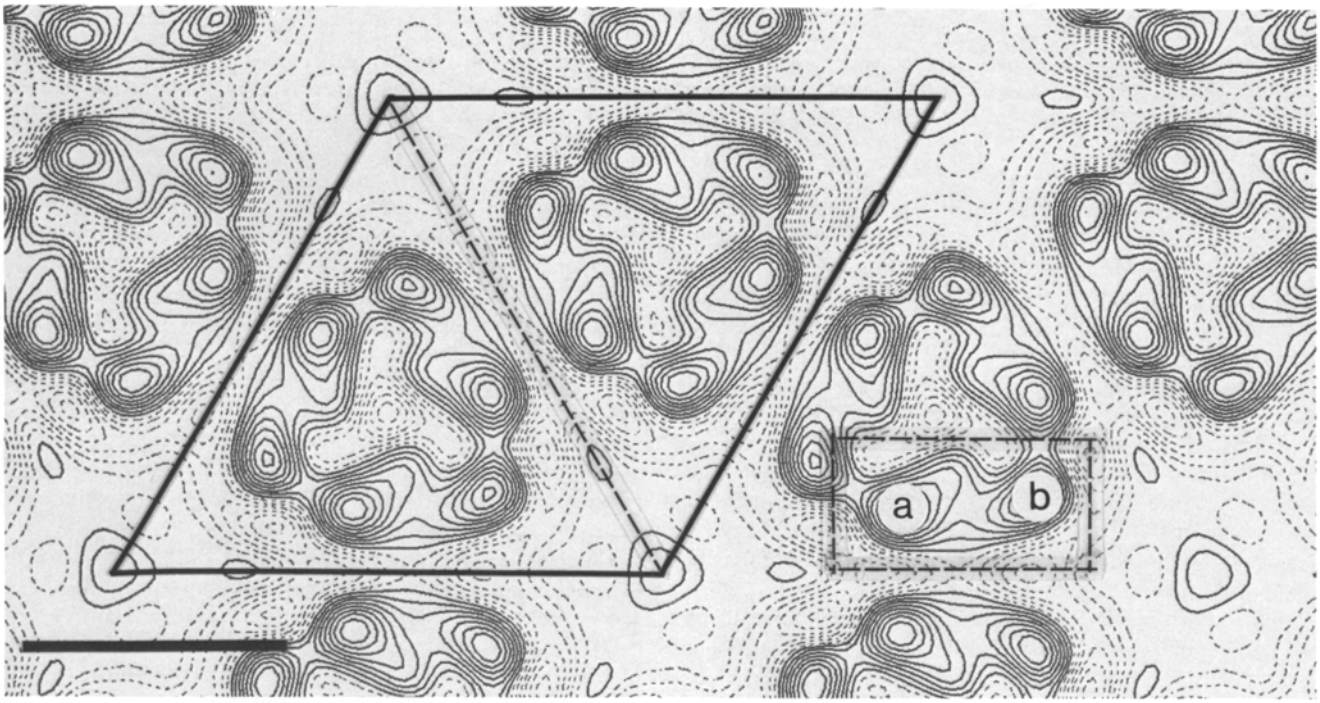


*Figure 9.* Projection map of averaged data at 17 Å resolution, with p321 symmetry imposed. A single unit cell (124 × 124 Å) is outlined with a solid line and the mirror plane within the unit cell is indicated by a dashed line. Each unit cell includes two oppositely facing trimers. The presumed monomer (outlined with a *dashed line*) consists of two domains of slightly different size (*a* and *b*). Bar, 60 Å.

4. Bürgi, R., F. Suter, and H. Zuber. 1987. Arrangement of the light-harvesting chlorophyll a/b protein complex in the thylakoid membrane. *Biochim. Biophys. Acta.* 890:346–351.
5. Burke, J. J., C. L. Ditto, and C. J. Arntzen. 1978. Involvement of the light-harvesting complex in cation regulation of excitation energy distribution in chloroplasts. *Arch. Biochem. Biophys.* 187:252–263.
6. Darr, S. C., S. C. Somerville, and C. J. Arntzen. 1986. Monoclonal antibodies to the light-harvesting chlorophyll a/b protein complex of photosystem. II. *J. Cell Biol.* 103:733–740.
7. Delepelaire, P., and N. H. Chua. 1981. Electrophoretic purification of chlorophyll a/b-protein complexes from *Chlamydomonas reinhardtii* and spinach and analysis of their polypeptide compositions. *J. Biol. Chem.* 256:9300–9307.
8. Dunahay, T. G., G. Schuster, and L. A. Staehelin. 1987. Phosphorylation of spinach chlorophyll-protein complexes. *FEBS (Fed. Eur. Biochem. Soc.) Lett.* 215:25–30.
9. Dunsmuir, P., S. M. Smith, and J. Bedbrook. 1983. The major chlorophyll a/b binding protein of petunia is composed of several polypeptides encoded by a number of distinct nuclear genes. *J. Mol. Appl. Genet.* 2: 285–300.
10. Hayat, M. A. 1970. Osmium tetroxide. *In* Principles and Techniques of Electron Microscopy. Van Nostrand Reinhold Co., Inc., New York. 36–44.
11. Henderson, R., and P. N. T. Unwin. 1975. Three-dimensional model of purple membrane obtained by electron microscopy. *Nature (Lond.).* 257:28–32.
12. Henderson, R., J. M. Baldwin, K. H. Downing, J. Lepault, and F. Zemlin. 1986. Structure of purple membrane from *Halobacterium halobium*: recording, measurement and evaluation of electron micrographs at 3.5 A resolution. *Ultramicroscopy.* 19:147–178.
13. Karlin-Neumann, G. A., B. D. Kohorn, J. P. Thornber, and E. M. Tobin. 1985. Chlorophyll a/b-protein encoded by a gene containing an intron with characteristics of a transposable element. *J. Mol. Appl. Genet.* 3:45–61.
14. Kühlbrandt, W. 1984. Three-dimensional structure of the light-harvesting chlorophyll a/b-protein complex. *Nature (Lond.).* 307:478–480.
15. Kühlbrandt, W. 1987. Three-dimensional crystals of the light-harvesting chlorophyll a/b protein complex from pea chloroplasts. *J. Mol. Biol.* 194:757–762.
16. Kühlbrandt, W., T. Thaler, and E. Wehrli. 1983. The structure of membrane crystals of the light-harvesting chlorophyll a/b protein complex. *J. Cell Biol.* 96:1414–1424.
17. Laemmli, U. K. 1970. Cleavage of structural proteins during the assembly of the head of bacteriophage T4. *Nature (Lond.).* 227:680–685.
18. Larsson, U. K., and B. Andersson. 1985. Different degrees of phosphorylation and lateral mobility of two polypeptides belonging to the light-harvesting complex of photosystem II. *Biochim. Biophys. Acta.* 809: 396–402.
19. Li, J. 1985. Light harvesting chlorophyll a/b-protein: three-dimensional structure of a reconstituted membrane lattice in negative stain. *Proc. Natl. Acad. Sci. USA.* 82:386–390.
20. Li, J., and C. Hollingshead. 1982. Formation of crystalline arrays of chlorophyll a/b-light-harvesting protein by membrane reconstitution. *Biophys. J.* 37:363–370.
21. Milligan, R. A., A. Brisson, and P. N. T. Unwin. 1984. Molecular structure determination of crystalline specimens in frozen aqueous solutions. *Ultramicroscopy.* 13:1–10.
22. Mullet, J. E. 1983. The amino acid sequence of the polypeptide segment which regulates membrane adhesion (grana stacking) in chloroplasts. *J. Biol. Chem.* 258:9941–9948.
23. Murphy. D. J. 1986. The molecular organization of the photosynthetic membranes of higher plants. *Biochim. Biophys. Acta.* 864:33–94.
24. Nabedryk, E., S. Andrianambinintsoa, and J. Breton. 1984. Transmembrane orientation of α-helices in the thylakoid membrane and in the light-harvesting complex. *Biochim. Biophys. Acta.* 765:380–387.
25. Plumley, F. G., and G. W. S. Schmidt. 1987. Reconstruction of chlorophyll a/b light-harvesting complexes: xanthophyll-dependent assembly and energy transfer. *Proc. Natl. Acad. Sci. USA.* 84:146–150.
26. Schoch, S., and J. Brown. 1987. The action of chlorophyllase on chlorophyll-protein complexes. *J. Plant Physiol.* 126:483–494.
27. Siefermann-Harms, D., and H. Ninnemann. 1982. Pigment organization in the light-harvesting chlorophyll a/b complex of lettuce chloroplasts. *Photochem. Photobiol.* 35:719–731.
28. Suss, K. H., O. Schmidt, and O. Machold. 1976. The action of proteolytic enzymes on chloroplast thylakoid membranes. *Biochim. Biophys. Acta.* 448:103–113.
29. Tapie, P., P. Haworth, G. Hervo, and J. Breton. 1982. Orientation of the pigments of the thylakoid membrane and in the isolated chlorophyll-protein complexes of higher plants. *Biochim. Biophys. Acta.* 682:339–344.
30. Thon, F. 1966. Zur Defokussierungsabhaengigkeit des Phasenkontrastes bei der elekronenmikroskopischen Abbildung. *Z. Naturforsch. Sect. C. Biosci.* 21a:476–478.
31. Thornber, J. P. 1975. Chlorophyll-proteins: light-harvesting and reaction center components of plants. *Annu. Rev. Plant Physiol.* 26:127–158.
32. Unwin, P. N. T., and P. D. Ennis. 1984. Two configurations of a channel-forming membrane protein. *Nature (Lond.).* 307:609–613.